

ABSOLUTE AND CONVECTIVE INSTABILITY OF SMITH-PURCELL FREE ELECTRON LASER

D. Li[#], K. Imasaki, ILT, 2-6 Yamada-oka, Suita, Osaka 565-0871, Japan
 Z. Yang, UEST, Chengdu, 610054, P.R.China
 Gun-Sik Park, SNU, Seoul 151-747, Korea

S. Miyamoto, S. Amano, T. Mochizuki, LASTI, 3-1-2 Koto, Kamigori, Hyogo 678-1205, Japan.

Abstract

The effect of dissipative loss in the grating surface on the Smith-Purcell free-electron laser is investigated with the help of a two-dimensional particle-in-cell simulation. The simulation model supposes an open aluminium grating driven by a continuous electron beam. With the present parameters, it has been shown that such a device can oscillate on both the convective and absolute instability when ignoring the surface-loss. The growth rate is found to be dependent of the beam energy, and it decreases when the surface-loss is involved. The results are compared with the recent theory.

INTRODUCTION

As a promising alternative in the development of a compact, tuneable and powerful THz source, the Smith-Purcell free-electron laser (SP-FEL) has attracted many attentions in recent years [1-5]. The SP-FEL can be realized on the configuration of an open grating [6-10], which is different from the conventional configuration, "orotron" or "ledatron" [11,12].

When an electron passes close to the surface of the grating, it not only emits Smith-Purcell radiation, but also excites the evanescent wave [13,14]. The evanescent wave, with the frequency below the lowest frequency of the Smith-Purcell radiation, travels along the grating and undergoes partial diffraction and partial reflection at both ends of the grating. The diffraction portion is radiative in the free space and can be utilized. The dispersion relation of the evanescent wave, as shown in Fig. 1, is similar to the backward-wave oscillators (BWOs) and traveling-wave tubes (TWTs), since the grating could be regarded as a kind of slow-wave structure. The frequency of the evanescent wave is determined from the intersection point of the dispersion curve and the beam line, as shown in Fig. 1, meaning that the beam velocity is synchronous with the phase velocity of the wave. The group velocity can be positive, negative or zero. When the interaction happens in the positive group velocity, the wave and the beam moves in the same direction. Such an interaction induces convective instability, and the device operates in the manner of TWTs [15]. When the group velocity is negative, the wave and the beam moves in the opposite direction. In this case, the interaction leads to absolute instability, and the device can operate without external feedback, like BWOs [15].

The case of absolute instability has been much

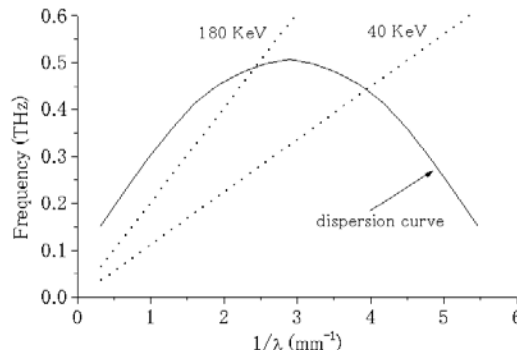


Figure 1: Dispersion relation for our grating.

addressed [6-9]. Andrews and co-workers predicted that there is possibility for device to start oscillation based on the convective instability, since the wave reflects at both ends of the grating, playing the role of external feedback [15]. In this paper, we address on the oscillation induced by absolute and convective instability, respectively, with the help of a two-dimensional particle-in-cell code, MAGIC [16], a code for simulating processes involving interactions between space charge and electromagnetic fields. The simulation is performed with and without involving the surface-loss of the grating, respectively, to demonstrate the effect of the loss on the operation of the device.

SIMULATION DESCRIPTION

The simulation geometry is shown in Fig. 2. A grating with rectangular form is set in the centre of the bottom of the simulation box. The surface of the grating is assumed to consist of conductor whose grooves are

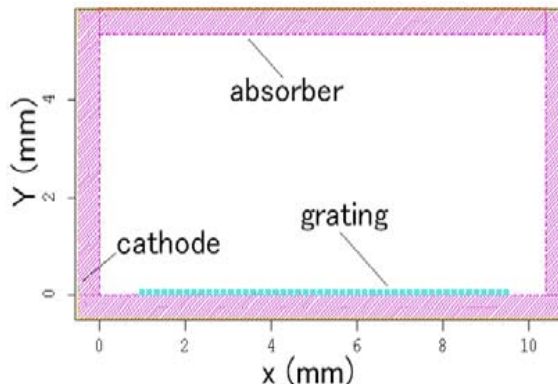


Figure 2: Simulation geometry.

[#]dazhi_li@hotmail.com

parallel and uniform in the z direction. We use a sheet electron beam with thickness of $24 \mu\text{m}$, and place its edge $34 \mu\text{m}$ above the top of the grating. It is a perfect laminar beam produced by the MAGIC algorithm and is generated from a cathode located at the left boundary of the simulation box. The electron-wave interaction and radiation propagation happen in the vacuum area, which is enclosed by a special region (called *free-space* in MAGIC language), where the incident electromagnetic waves and electrons can be absorbed. The whole simulation area is divided into a mesh with rectangle cells of small size ($\delta x=17.3 \mu\text{m}$, $\delta y=17.3 \mu\text{m}$) in the region of beam propagation and grating, and large size ($\delta x=17.3 \mu\text{m}$, $\delta y=51.9 \mu\text{m}$) in the rest of the region. The Cartesian coordinate system is adopted with the origin at the centre of the grating. Since it is a two-dimensional simulation, it assumes that all fields and currents are independent of the z coordinate. And it should be noted that the current value mentioned in this paper represents the current per meter in the z direction.

The main parameters of the grating and electron beam are summarized in table 1. The electron beam

Table 1 Main parameters for simulation

Grating period	$L=173 \mu\text{m}$
Groove width	$w=62 \mu\text{m}$
Groove depth	$d=100 \mu\text{m}$
Period number	$N=50$
Electron beam energy	$E=40 \sim 140 \text{ KeV}$
Beam current	$I=648 \text{ A/m}$
Beam thickness	$\sigma=24 \mu\text{m}$
Beam-grating distance	$\delta=34 \mu\text{m}$
External magnetic field	$B_x=2 \text{ T}$

energy will be varied in the following simulation. The external magnetic field is used in order to ensure stable beam propagation above the grating. It should be noted that some parameters of the grating and electrons, such as period length, groove depth and width, and electron's energy, used in our simulation are the same as those in Dartmouth experiment [1]. Consequently the radiation occurs in the THz regime. However, the grating length in our simulation is shorter than the one used in Dartmouth

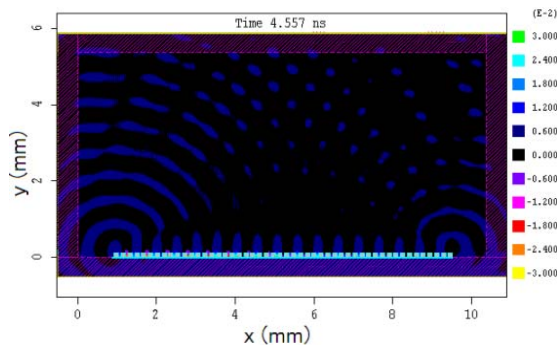


Figure 3: Contour plot of B_z for the case of 50 KeV electron beam.

experiment because of the limited capacity of our computers. In addition, the form of the beam is different, since we use a sheet beam and the experiment used a round beam.

As to the diagnostics, MAGIC allows us to observe a variety of physical quantities such as electromagnetic fields as functions of time and space, power outflow, and electron phase-space trajectories [16]. We can set the relevant detectors anywhere in the simulation area.

SIMULATION RESULTS

Ignoring Surface-loss

We first perform the simulation at the ignorance of the surface loss, i.e., the grating is supposed to be perfect conductor. The choice of beam energy spans the regions of absolute and convective instability. According to the theory of Andrews and Brau, the beam line intersects the point of zero group velocity, called Bragg condition, with the energy of 125 keV [15]. Fig.3 and 4 show the contour plot of B_z and energy modulation for the beam energy of 50 keV, at the time of 4.703 ns. In this case, the device operates on the absolute instability, and the energy modulation tells that the oscillation happens. If the beam energy is 140 keV, the device operates on the convective instability. From Fig. 5 we understand that the ends of the grating reflect the wave, and therefore provide feedback.

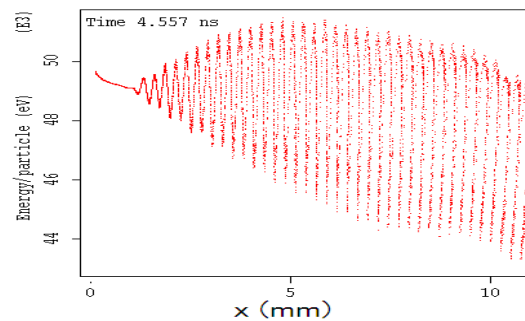


Figure 4: Energy modulation for the case of 50 keV electron beam.

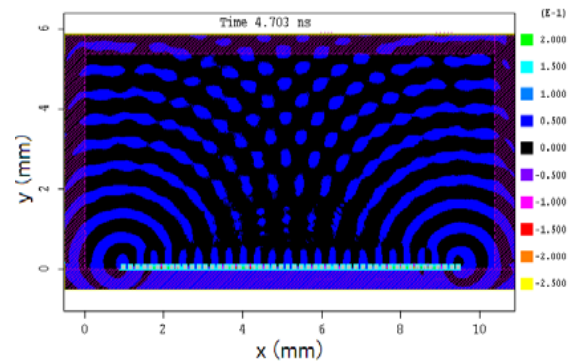


Figure 5: Contour plot of B_z for the case of 140 KeV electron beam.

The reflected waves form the interference pattern. Fig. 6 illustrates the modulation of the energy, meaning that the

device oscillates. The electric field component of the evanescent wave is observed near the grating surface, as examples, simulation results for some chosen energies are given in Fig.7. It is seen that the evolution of the

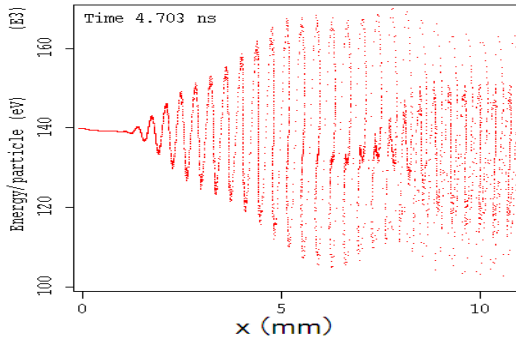


Figure 6: Energy modulation for the case of 140 keV electron beam.

amplitude of the electric field component in the x direction shows the exponential growth for all chosen energy, which means the device can oscillate by both absolute and convective instability, even at the Bragg condition. We noticed that when the beam energy is 125 KeV or more, the curves illustrate several sharp decreases as the amplitude growing.

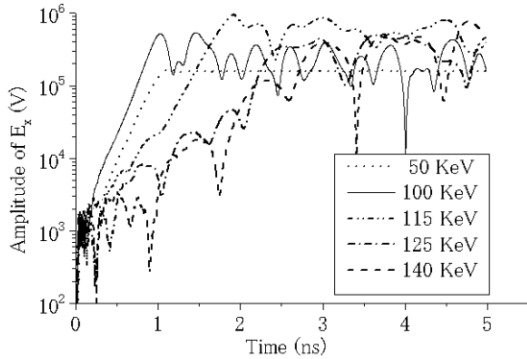


Figure 7: Evolution of amplitude of E^x with respect to time.

Involving Surface-loss

To be more practical, the grating should not be perfect conductor and it has loss in the surface. In this paper, we consider aluminium grating, which has the conductivity of 3.72×10^7 mhos/m. With involving the surface-loss, the evolution of the electric field amplitude corresponding to Fig.7 is as shown in Fig.8. It is understood that only the curves for 50KeV, 100KeV and 115KeV (operating on absolute instability) demonstrate the exponential growth, while for the case of 140KeV electron beam (operating on convective instability) the oscillation refuses starting. Further analysis of the simulation data shows that with the present parameters the device can only oscillate on the absolute instability. Comparing with Fig.7, the curve of 50KeV comes to saturation ahead of the curve of 100KeV in Fig. 8, which

means the effect of surface loss strongly depends on the beam energy.

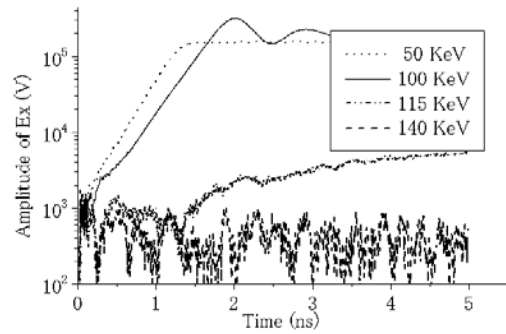


Figure 8: Evolution of amplitude of E_x with respect to time.

Growth rate

The growth rate of the evanescent wave can be derived from the simulation data. From the plot of amplitude of $E_x(t)$ vs t we can extract the slope of the linear envelop, which is the imaginary part of the frequency, $Im(\omega)$ [9]. Plenty of simulations are carried out with the variation of electron beam energy, and the growth rate for the particular energy is acquired by the way described above. The dependency of growth rate on beam energy is illustrated in Fig.9, for the cases of with and without surface loss, respectively. It has been shown that, the growth rate decreases when the surface-loss is involved. With the present parameters, the maximum growth rate appears at the energy of ~ 65 KeV for the case of with surface loss, then it goes down quickly to zero before the Bragg condition. That is the reason that the device can only operate on the absolute instability. If we expect the device oscillate at the convective instability, much higher current of electron beam is required to get the net gain. Also plotted in Fig.9 are the theoretical results from the recent theory [17], which show about two times larger than the simulation results.

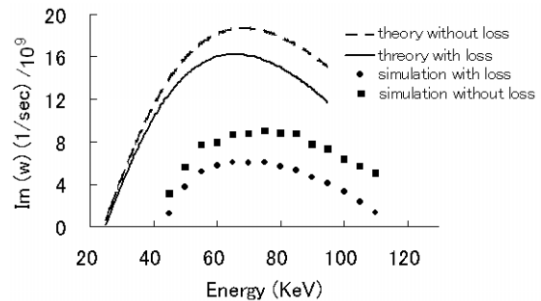


Figure 9: Growth rate with respect to beam energy.

CONCLUSION

The operation of a SP-FEL on absolute and convective instability is discussed in this paper. We demonstrate that the ends of the grating can provide the external feedback, which is possible to make the device oscillate at the

convective instability. The surface-loss will decrease the growth rate, especially in the region of convective instability. The growth rate drops down to zero before the Bragg condition with the present parameters. Higher beam current is predicted to provide the net gain if we expect the device to oscillate on the convective instability when the practical metal, such as aluminium, is used to make the grating.

ACKNOWLEDGMENTS

The authors gratefully acknowledge helpful discussions with Charles Brau and Heather Andrews.

REFERENCES

- [1] J. Urata, M. Goldstein, M. F. Kimmitt, A. Naumov, C. Platt, and J. E. Walsh, Phys. Rev. Lett. **80**, 516 (1998).
- [2] A. Bakhtyari, J. E. Walsh and J. H. Brownell, Phys. Rev. E **65**, 066503 (2002).
- [3] L. Schachter and A. Ron, Phys. Rev. A **40**, 876 (1989).
- [4] S.E.Korbly, A.S. Kesar, J.R.Sirigiri and R.J.Temkin, Phys. Rev. Lett. **94**, 054803, (2005).
- [5] K. -J. Kim and S. -B. Song, Nucl. Instrum. Methods Phys. Res., sect. A **475**, 158 (2001).
- [6] H. L. Andrews and C. A. Brau, Phys. Rev. ST Accel. Beams **7**, 070701 (2004).
- [7] H.L.Andrews, C.H.Boulware, C.A.Brau and J.D.Jarvis, Phys. Rev. ST Accel. Beams **8**, 110720 (2005).
- [8] V. Kumar and K.-J. Kim, Phys. Rev. E **73**, 026501 (2006).
- [9] J.T.Donohue and J.Gardelle, Phys. Rev. ST-AB, **8**, 060702 (2005).
- [10] J.T.Donohue and J.Gardelle, Phys. Rev. ST-AB, **9**, 060701 (2006).
- [11] R. P. Leavitt, D. E. Wortman, and C. A. Morrison, Appl. Phys. Lett. **35**, 363(1979)
- [12] K. Mizuno, S. Ono and Y. Shibata, IEEE Trans. Electron devices, ED-20, 749 (1973)
- [13] D.Li, Z. Yang,K.Imasaki and Gun-sik Park, Phys. Rev. ST-AB **9**, 040701 (2006)
- [14] D.Li, K.Imasaki , Z. Yang and Gun-sik Park, Appl. Phys. Lett. **88**, 201501 (2006)
- [15] H.L.Andrews, C.H.Boulware, , and J.D.Jarvis, Phys. Rev. ST Accel. Beams **8**, 050703 (2005).
- [16] L. Ludeking, The MAGIC user's manual.
- [17] C.A.Brau (private communication).